Synthesis and Theoretical Studies of a Double Helical Complex with the Ligand 4′,4′′′-Bis(ferrocenyl)-2,2′:6′,2′′:6′′,2′′′:6′′′,2′′′′-quinquepyridine

Javier E. Aguado,[a] Maria José Calhorda,[b] Paulo J. Costa,[b] Olga Crespo,[a] Vitor Félix,[c] M. Concepción Gimeno,[a] Peter G. Jones,[d] and Antonio Laguna*[a]

Keywords: Quinquepyridine / Silver / Helical complexes / Ferrocenyl derivatives / Theoretical studies

4′,4′′′-Bis(ferrocenyl)-2,2′:6′,2′′:6′′,2′′′:6′′′,2′′′′-quinquepyridine (Fc_2qpy) reacts with AgOTf (OTf = trifluoromethylsulfonate) to give a complex of stoichiometry [Ag(Fc2qpy)]-OTf. The crystal structure reveals a dinuclear arrangement among the cations with an Ag···Ag close contact of 3.089(2) Å. The ligands are wrapped around the silver atoms in a double helical array. Further hydrogen bonding between triflate units and the protons of the ferrocene or pyridine moieties results in a supramolecular structure. Theoretical studies confirm the existence of a weak Ag–Ag bond, and show that the dinuclear form can be more stable than the mononuclear one, when there is a favorable balance between the reorganization energy of the two quinquepyridine chains and the energy released by the formation of stronger Ag–N bonds and the new Ag–Ag interaction in the helix.

Introduction

The construction of inorganic supramolecular arrays based on covalent interactions, hydrogen bonding, or other intermolecular interactions is a very interesting area of functional materials.[1−6] Oligopyridines have been used as building blocks for the self-assembly of double helical transition-metal complexes.[3−6] The close proximity between the bipyridine or terpyridine units, which is essential for the formation of the double helical complexes, leads to substantial π-π interactions, but also to some constraints upon complex formation. 2,2′:6′,2′′:6′′,2′′′:6′′′,2′′′′-quinquepyridine (qpy) has a rich transition metal coordination chemistry because of its ability to promote tetrahedral, square planar or octahedral geometries.[7−31] There are several coordination modes, the important ones in the formation of metal helicates being those which lead to the partitioning of the ligand into bidentate and tridentate units. This happens, for example, with several first row transition metals. For metals that have no electronic preference for geometry, the assembly is dictated by the size of the metal ion and the available bonding cavity. For the quinquepyridine ligand in a planar configuration, Constable et al. have shown that the five nitrogen atoms form an effective hole-size ca. of 2.45 Å which corresponds to a pentagonal-planar geometry for metals with an ionic radius 1.0 ± 0.1 Å, and such a geometry has been demonstrated for silver(I) in the complex [Ag(qpy)]PF_6.[7] The introduction of sterically demanding substituents to the quinquepyridine can be expected to increase the effective hole-size of the bonding cavity. Consequently, silver(I) is too small to be accommodated by the ligand in a planar pentadentate mode, and supramolecular helical structures can then be achieved. There are few examples of doubly helical silver complexes with quinquepyridine ligands. In the complex $[Ag_2(dmpqpy)_2](ClO_4)_2 \cdot 2H_2O$ (dmpqpy = 6,6′′′′-dimethyl-4′,4′′′-diphenyl-2,2′:6′,2′′:6′′,2′′′:6′′′,2′′′′-quinquepyridine)[31] the ligand acts as tetradentate donor, and the central pyridine nitrogen atoms play the role of rigid spacers, rather than of donor atoms. The silver center is also tetracoordinate in the heterodinuclear derivative $[AgCo(qpy)_2]^{3+}$.[19] Pentacoordinated silver atoms are present in $[Ag_2(dmqpy)_2](ClO_4)_2$ (dmqpy = 6,6′′′′-dimethyl-2,2′:6′,2′′:6′′,2′′′:6′′′,2′′′′-quinquepyridine).[31]

Here we report on the synthesis of the Ag^I complex of the 4′,4′′′-bis(ferrocenyl)-2,2′:6′,2′′:6′′,2′′′:6′′′,2′′′′-quin-

[a] Departamento de Química Inorgánica, Instituto de Ciencia de Materiales de Aragón, Universidad de Zaragoza, C.S.I.C., 50009 Zaragoza, Spain
[b] ITQB, Av. da República, EAN, Apart. 127, 2781−901, Oeiras, and Departamento de Química e Bioquímica, Facultade de Ciências, Universidade de Lisboa, Campo Grande 1749−016 Lisboa, Portugal
[c] Departamento de Química, Universidade de Aveiro, CICECO, 3810−193 Aveiro, Portugal
[d] Institut für Anorganische und Analytische Chemie der Technischen Universität, Postfach 3329, 38023 Braunschweig, Germany
Supporting information for this article is available on the WWW under http://www.eurjic.org or from the author.

  DOI: 10.1002/ejic.200400057

quepyridine ligand. The crystal structure of the silver(I) derivative shows a double helical arrangement with a short Ag···Ag interaction. Both silver(I) atoms have slightly different geometries. One can be considered as pentacoordinate with an elongated trigonal bipyramidal geometry, and the other as tetracoordinate with a tetrahedral geometry. Theoretical studies have been carried out addressing the formation of the silver(I)-silver(I) interaction as well as the difference in energy between the mononuclear and the dinuclear complexes.

Results and Discussion

Synthesis

The ligand 4′,4′′′-bis(ferrocenyl)-2,2′:6′,2′′:6′′,2′′′:6′′′,2′′′′-quinquepyridine (Fc_2qpy) reacts with AgOTf to give a deep-red solution, from which a complex of stoichiometry [Ag(Fc_2qpy)]OTf was isolated. The X-ray structure confirms that the complex is in fact dimeric with a double helical structure [Equation (1)].

The positive liquid secondary-ion mass spectrum (LSIMS+) exhibits a peak at m/z = 863 (100%), which can be assigned to the cationic molecular peak $[Ag(Fc_2qpy)]^+$. No peaks corresponding to the dinuclear species $[Ag_2(Fc_2qpy)_2]^{2+}$ or $[Ag_2(Fc_2qpy)_2(OTf)]^+$ were detected. The ^{1}H NMR spectrum of [Ag(Fc_2qpy)]OTf shows the signals arising from the protons of the ferrocenyl moieties at δ = 4.12, 4.63, and 4.95 ppm in a ratio 10:4:4. This corresponds to the unsubstituted cyclopentadienyl, and to the α and β protons of the substituted cyclopentadienyl groups, respectively. Five multiplets arise from the quinquepyridine protons, although some of them are overlapping.

Crystal Structure of [Ag(Fc_2qpy)]OTf

The crystal structure of $[Ag\{Fc_2(qpy)\}]_2(OTf)_2 \cdot 3CH_2Cl_2$ has been determined by X-ray diffraction (Figure 1). A selection of bond lengths and angles appears in Table 1. The cation displays a double-helical arrangement, achieved by a series of twists. The dihedral angles between adjacent pyridine planes 8 and 7 (9.5°), 7 and 6 (28.4°), 6 and 9 (38.6°), and 9 and 10 (5°) in one ligand, and between planes 5 and 4 (3.5°), 4 and 1 (32°), 1 and 2 (35.5°), and 2 and 3 (14.2°) in the other (planes are numbered after the nitrogen atoms they contain) confirm that the major twisting in each ligand occurs between the central pyridyl ring and the 2,2′-bipyridyl fragments.

The twisting can be seen more clearly from the space-filling diagram (Figure 2). The helical radius is about a/3,

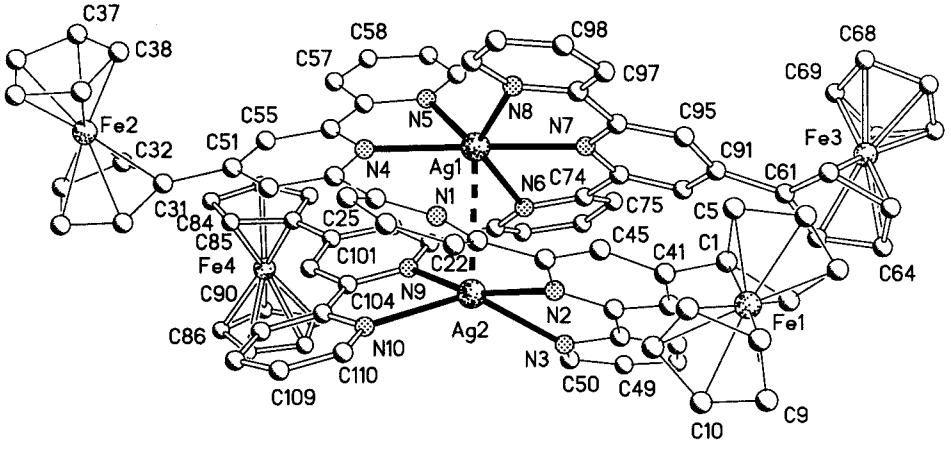

Figure 1. Structure of the cation of $[Ag_2(Fcqpy)_2](OTf)_2$

Table 1. Selected bond lengths (Å) and angles (°) for compound $[Ag_2(Fc_2qpy)_2](OTf)_2$

Ag(1)−N(7)	2.323(9)	Ag(1)−Ag(2)	3.089(2)
Ag(1)−N(4)	2.341(9)	Ag(2)−N(2)	2.329(9)
Ag(1)−N(5)	2.395(11)	Ag(2)−N(9)	2.341(9)
Ag(1)−N(8)	2.516(11)	Ag(2)−N(10)	2.376(10)
Ag(1)−N(6)	2.550(10)	Ag(2)−N(3)	2.418(11)
N(7)−Ag(1)−N(4)	169.2(3)	N(8)−Ag(1)−Ag(2)	118.1(3)
N(7)−Ag(1)−N(5)	119.7(3)	N(6)−Ag(1)−Ag(2)	61.1(2)
N(4)−Ag(1)−N(5)	70.0(4)	N(2)−Ag(2)−N(9)	161.7(4)
N(7)−Ag(1)−N(8)	68.8(3)	N(2)−Ag(2)−N(10)	123.5(3)
N(4)−Ag(1)−N(8)	102.3(3)	N(9)−Ag(2)−N(10)	71.2(3)
N(5)−Ag(1)−N(8)	124.1(4)	N(2)−Ag(2)−N(3)	69.7(4)
N(7)−Ag(1)−N(6)	68.9(3)	N(9)−Ag(2)−N(3)	108.3(3)
N(4)−Ag(1)−N(6)	119.5(3)	N(10)−Ag(2)−N(3)	135.7(4)
N(5)−Ag(1)−N(6)	80.2(3)	N(2)−Ag(2)−Ag(1)	86.3(3)
N(8)−Ag(1)−N(6)	137.6(3)	N(9)−Ag(2)−Ag(1)	78.3(3)
N(7)−Ag(1)−Ag(2)	91.8(3)	N(10)−Ag(2)−Ag(1)	107.8(3)
N(4)−Ag(1)−Ag(2)	87.1(3)	N(3)−Ag(2)−Ag(1)	115.6(3)
N(5)−Ag(1)−Ag(2)	116.7(3)		

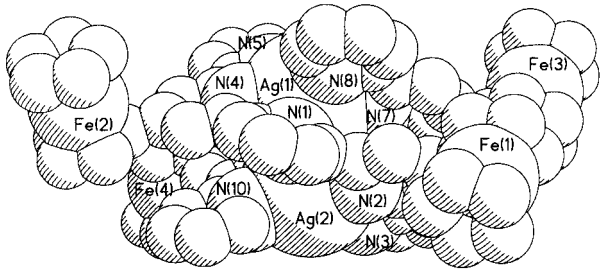

Figure 2. Space filling diagram of the cation in $[Ag_2(Fcqpy)_2](OTf)_2$

4.5 Å and the pitch height about *a*/2, 7 Å. A very distorted trigonal bipyramidal disposition results for one silver atom, upon coordination to three nitrogen atoms of one [Fc_2qpy] ligand, and two from the other [equatorial Ag−N distances 2.323(9), 2.341(9), 2.395(11) Å, axial 2.516(11), 2.550(10) Å]. The atoms N4, N5, N7, and Ag1 lie in the same plane, and the angle between this plane and the plane N8, N6, N7, Ag1 is 60.2°. The other silver atom is bonded to two nitrogen atoms from each ligand. This four-coordinate metal center [Ag−N distances 2.329(9)−2.418(11) Å] shows a very irregular geometry. The dihedral angle between planes N9−Ag2−N10 and N2−Ag2−N3 is 55.3°. This points to a geometry intermediate between tetrahedral and square planar. Thus, in this complex, the two silver(I) atoms exhibit different coordination modes to the quinquepyridine moieties. This is unprecedented since, in metal complexes with this type of ligand, the same coordination has always been observed for both metal ions, for example in $[M_2X(qpy)]^{3+}$ (M = Cu, Co, Ru),[9,10,13,20] or $[M_2X\{(SMe)_2qpy\}_2]^{3+}$ (M = Cu, Ni),[28,29] where the metallic centers are hexacoordinate. Only in complexes which contain two metals in different oxidation states, such as in $[Cu_2(R_2qpy)_2]^{3+}$ (R = SMe, Ph),[28,30] is it possible to find different geometries. Here Cu^{I} is tetrahedral, whereas Cu^{II} is octahedral.

Despite the covalence of the bonding to each silver atom in the compound, the Ag−N distances are within the expected range. The Ag(1)···Ag(2) contact of 3.089(2) Å in $[Ag_2(Fc_2qpy)_2](OTf)_2$ is shorter than in the related examples with qpy derivatives, i.e. 3.48 Å in $[Ag(dmqpy)_2](ClO_4)_2$,[31] and 3.22 Å in $[Ag(dmpqpy)_2](ClO_4)_2\cdot 2H_2O$,[31] but close to those found in complexes with ligands based on terpyridine (terpy) or quaterpyridine (qtpy) units, e.g. $[Ag_2(qtpy)_2](BF_4)_2$ [3.107(2) Å],[34] and $[Ag_2(terpy)_2](PF_6)_2$ (2.914−2.940 Å in each double helical di-silver unit, Ag···Ag contacts of 3.107, 3.156 Å with a second dinuclear unit to form tetranuclear blocks).[33] The distances of the silver atoms Ag1 or Ag2 to the same silver atoms of different units are 7.47 and 6.57 Å, respectively. In $[Ag_2(Fc_2qpy)_2](OTf)_2$ the twisting angles are smaller than in the silver derivatives $[Ag_2(dmqpy)_2](ClO_4)_2$,[31] (major twist angle 47.2°, between terpyridyl and bipyridyl fragments) or $[Ag(dmpqpy)_2](ClO_4)_2\cdot 2H_2O$ (major twist angles 36.8°, 36.1°, in this case between the two bipyridyl fragments and the central ring).[31] These values are in accordance with a shorter silver···silver contact. It has been suggested that it is the steric effect of the terminal groups in flexible ligands with various donor atoms that forces the ligand to adopt a double helical disposition, since the planar configuration is not possible. Four factors seem to govern the formation of a double helical complex, namely the ligand donor set, the coordination geometry of the metal ion, the metal-ion radius, and the substituent effects. These three helical complexes allow an analysis of the effect of the substituents, since the ligand (qpy) and the metal ion (Ag^+) are common to all. The bulkier ferrocene moiety affords the smallest twist angles and, thus, the shortest silver···silver interaction. The presence of four substituents (methyl and phenyl) in qpy, in the 6,6′′′′ and 4′,4′′′ positions, produces a milder effect in the twisting of the ligand than the case with only two ferrocene substituents in the 4′,4′′′ positions.

Stacking interactions between the planar parts of the ligands, reminiscent of the base-pair stacking of nucleic acids, are usual in these helical geometries, sometimes as marked interactions. In $[Ag_2(Fc_2qpy)_2](OTf)_2$ the rings that contain the nitrogen atoms N7 and N2 are almost coplanar (angle between planes 7°), and one lies approximately above the other. The same situation can be observed for the planes that contain N9 and N4 (angle between the planes = 5.6°). The distances between the ring centroids are 3.43 Å and 3.98 Å, respectively. The shorter distance is similar to the stacking distances in $[Ag_2(dmqpy)_2](ClO_4)_2$ (3.38−3.42 Å), and the larger distance is similar to those between di-silver units in the same compound (3.70 Å).[31] No such interactions were observed between di-silver units, since the rings of those which are adjacent are not coplanar. These interactions between di-units are not present in $[Ag(dmpqpy)_2](ClO_4)_2\cdot 2H_2O$, probably due to the presence of the bulky substituents.

Helices are chiral although, normally, a mixture of both enantiomers is obtained, and only the presence of a chiral substituent makes it possible to obtain only one enantiomer. In $[Ag_2(Fc_2qpy)_2](OTf)_2$, the two enantiomers are alternately (Figure 3) disposed. The presence of C−H···O and C−H···F hydrogen bonds (Table 2) results in a supramolecular structure.

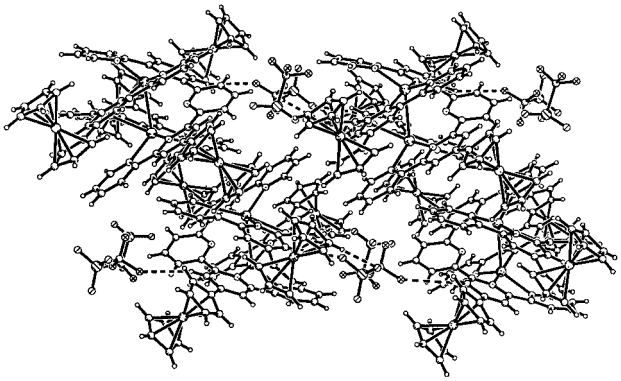

Figure 3. Packing diagram of $[Ag_2(Fcqpy)_2](OTf)_2$

Table 2. Hydrogen bonds [Å and °]

D−H···A	*d*(D−H)	*d*(H···A)	*d*(D···A)	<(DHA)
C(35)−H(35)···O(2)	0.95	2.58	3.415(15)	147.3
C(52)−H(52)···O(2)	0.95	2.54	3.459(16)	162.7
C(25)−H(25)···O(3)	0.95	2.51	3.152(15)	124.7
C(75)−H(75)···O(4)#1	0.95	2.58	3.415(15)	146.7
C(92)−H(92)···O(4)#1	0.95	2.48	3.372(16)	157.3
C(70)−H(70)···O(5)#1	0.95	2.54	3.490(19)	174.3
C(22)−H(22)···F(6)#2	0.95	2.46	3.198(16)	134.1

Symmetry transformations used to generate equivalent atoms: #1: $-x, -y + 1, -z$, #2: $-x + 1, -y + 1, -z$

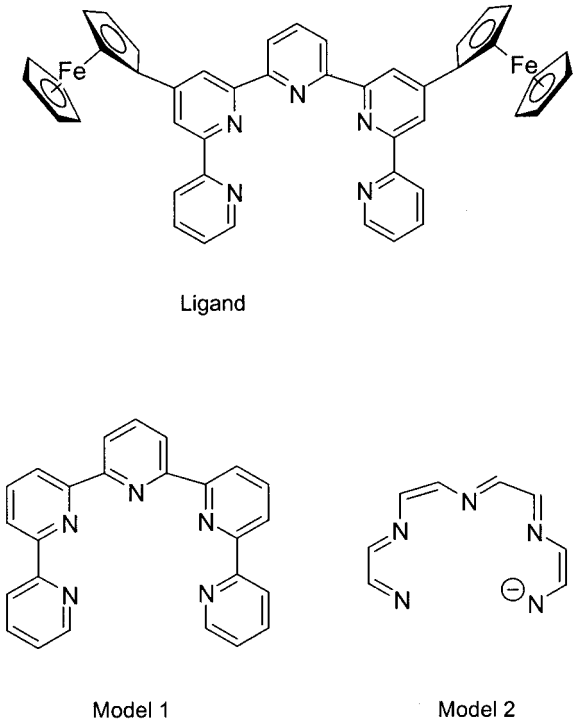

Scheme 1. Theoretical models

Electrochemistry

The electrochemical behavior of the silver complex has been studied by cyclic voltammetry at a platinum electrode in CH_2Cl_2. It shows two oxidation waves. The first is a quasi-reversible two-electron oxidation wave at +0.6 V based on the ferrocene units, a potential slightly higher than that of the free ferrocene (0.47 V). The second is an irreversible oxidation wave at +1.1 V attributable to the oxidation of the silver(I) to silver(II). These reduction waves overlap at around +0.4 V.

Theoretical Studies

Theoretical calculations were performed in order to understand the factors leading to the helical structure observed, and to establish the nature of the Ag···Ag interaction. Several approaches were used, taking into account the size of the system and the adequacy of the method. Geometry optimizations were mainly performed using DFT[34] methods (ADF program[35]), although HF (Gaussian 98[36]) was also tested. Single point MP2[37] calculations were carried out in order to account for correlation effects in the Ag···Ag interactions. The complete structure consists of a large number of atoms, so that models had to be built in such a way as to preserve the features of the experimental structure. For instance, the ferrocenyl units are directed toward the outside of the helices, and were therefore removed. The pyridines were also simplified, keeping the same bonding modes, which implied changing the charge. These models are shown in Scheme 1.

Model 1 was used in a molecular dynamics study of the isolated ligands, aimed at measuring the tendency of the two ligands to preserve the helical arrangement even in the absence of the metal. Model 2 was used in all the quantum calculations.

The quality of the model was addressed first. The structure with two chains and two silver atoms was fully optimized (ADF program; for details see Exp. Sect.). In Figure 4,

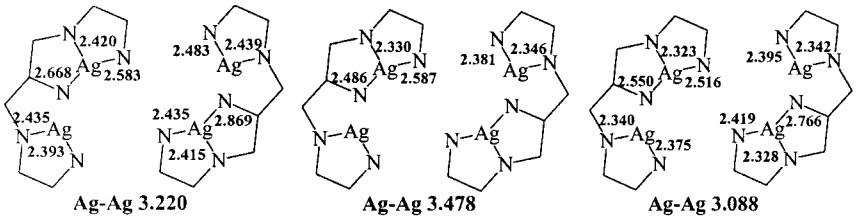

Figure 4. Ag−N distances (Å): calculated using DFT methods (left); in the X-ray structure of $[Ag_2(Fc_2qpy)_2]^{2+}$ (center); in the X-ray structure of $[Ag_2(dmqpy)_2]^{2+}$ (right)

we show a comparison of the calculated Ag−Ag and Ag−N distances (Å) with those found in the corresponding section of the experimental structure of the $[Ag_2(Fc_2qpy)_2]^{2+}$ helix (notice that for clarity, silver atoms are represented twice, as each chain binds two silvers), and also of the $[Ag_2(dmqpy)_2]^{2+}$ complex (owing to symmetry, only one set of distances is given).[31]

Although the Ag−Ag distance is either slightly too long or too short, depending on the structure considered, some Ag−N distances compare relatively well. Each helix binds two different Ag atoms, using three N atoms for the first Ag, and two N atoms for the second. One of the Ag−N distances in each chain is too long for a bond (2.869, 2.668 Å, and 2.766, 2.550 Å, respectively, for the calculated and experimental distances of $[Ag_2(Fc_2qpy)_2]^{2+}$). A similar binding mode was found in the $[Ag_2(dmqpy)_2]^{2+}$ complex (TEPDUN; there is another complex with the same stoichiometry but a less similar environment). The agreement with respect to distances appears acceptable. The helical arrangement is also retained in this simple model, as can be seen in Figure S1 (See Supporting Information, for Supp. Inf. see also the footnote on the first page of this article).

In the following step, we separated the two chains from the original structure, as shown in Scheme 2, and allowed each fragment to relax in order to optimize the structure.

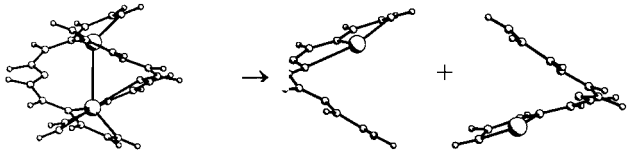

Scheme 2. Separation of the two fragments

The optimized structure consists of an almost flat pentacoordinate Ag complex of the qpy ligand, very similar to the X-ray structure of $[Agqpy]^+$, and is shown in Figure 5.

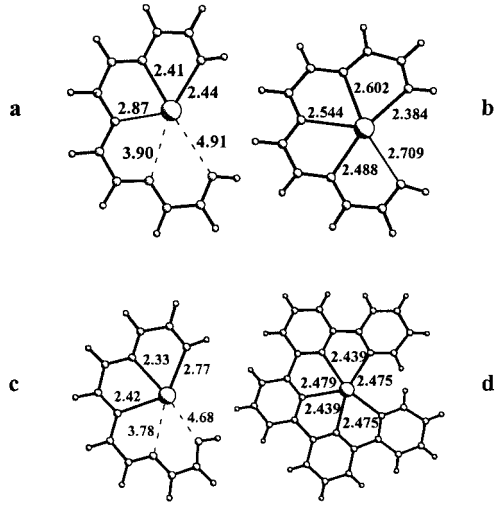

Figure 5. Structures containing one ligand chain and one silver atom: optimized in the helical structure of $[Ag_2(Fc_2qpy)_2]^{2+}$ (a), optimized alone (b), cut from the X-ray structure of the $[Ag_2(Fc_2qpy)_2]^{2+}$ helix (c), X-ray structure of the $[Agqpy]^+$ complex (d).

The Ag−N bond lengths are quite different from those in the helix, also shown in Figure 5, but very close to the distances in the $[Agqpy]^+$ complex, with the exception of one very long bond. Both in the calculated and the experimental helices, there are two Ag−N distances outside the bonding range (3.62, 4.65, or 3.90, 4.91, in the X-ray and calculated structures, respectively). Silver forms extra bonds with nitrogen atoms from the second chain. When the second chain is absent, the five possible Ag−N bonds are formed, and the energy decreases significantly (166 kcal mol^{-1}). How does the formation of the helical structure compete with the formation of two pentacoordinate monomers? Using the ADF optimized structures, we also performed single point HF and MP2 calculations on the monomer, the dimer, and the observed structure. The binding energy of the helical species relative to the sum of the energies of the single chains with the structure they have in the helix (see a in Figure 5) is represented by ΔE_1, and follows directly from Scheme 2. ΔE_2 represents the binding energy relative to two optimized single chains (see b in Figure 5). The difference between these two terms reflects the reorganization energy of each chain from flat to helical, and will be discussed again later. These binding energies are shown in Table 3.

Table 3. Binding energies (kcal·mol^{-1}) of the optimized helical structures relative to the monomer with the geometry in the optimized helical structure (ΔE_1) and the optimized AgL monomer (ΔE_2)

	DFT(ADF)	HF	MP2
ΔE_1	−51.1	−40.4	−90.4
ΔE_2	−5.9	8.5	−26.8

The ΔE_1 values are less relevant, since they give us the interaction energy for adding together the two chains shown in Scheme 2. They are always negative indicating that the formation of the four extra Ag−N bonds (each chain makes two bonds to the second silver atom), and eventually the new Ag−Ag bond, is an exothermic process. ΔE_2 values are much more interesting, because they include the reorganization energy of going from the flat pentacoordinate complex to a helix. This energy may be compensated for by stronger Ag−N bonds (same number, but organized differently) and a new Ag−Ag interaction. HF values give a positive energy, meaning that the helical structure is not favorable. On the other hand, both DFT and MP2 results agree on the higher stability of the double helix relative to the flat monomer, the interaction energy being larger in the MP2 calculation. This indicates that there is some weak Ag−Ag interaction, which relies on correlation and other effects, which are not all described by HF methods, but are fully taken into account by MP2, and only partly by the DFT functionals used. In the absence of this Ag−Ag interaction, the double helix is not favored, which follows from the HF data. Introduction of correlation (DFT) leads to the detection of the Ag−Ag interaction. A better description of cor-

relation by MP2 increases the exothermiticity of the process.

The existence of the Ag−Ag interaction can be further probed by indicators of bond strength, such as overlap populations or related indices. The experimental distance is relatively long (3.09 Å). Therefore, we performed a natural population analysis,[38] and calculated Wiberg[39] and Mayer[40,41] indices. The Wiberg index, calculated with the MP2 method, was 0.022 for both the optimized structure (model 2) and the $[Ag_2(Fc_2qpy)_2]^{2+}$ helix, indicating a weak bond. The Mayer index, a generalization of the Wiberg index calculated by the ADF program, led to values of 0.066 and 0.086 for the optimized structure and the helix, respectively. These results are all consistent with the existence of a weak Ag···Ag interaction. We may therefore conclude that the helical structure can become energetically more favorable than the existence of monomers, owing to the strong Ag−N bonds that can also be formed in this arrangement, and the extra development of a metal−metal interaction. There is a balance between these terms and the reorganization energy of each chain, which opposes helix formation.

After analyzing the preferences of silver, we address the preferences of the chain in the absence of silver, by means of molecular mechanics and dynamics simulations using the Universal Force Field,[42] within the Cerius2 software package.[43]

A conformational analysis of a single qpy chain (model 1) was undertaken following quench dynamics techniques at 3000 K. The five pyridine rings can adopt *cis* or *trans* arrangements, depending of values of the N−C−C−N torsion angles between adjacent pyridine rings. When the two nitrogen atoms of two contiguous pyridines are opposite to each other, with an almost co-planar arrangement of the aromatic rings, the N−C−C−N torsion angle is near 180°, and the configuration is *trans* (*t*). If they are on the same side, the N−C−C−N torsion angle is near 0°, and the configuration is *cis* (*c*). Apart from changes in the signs of the torsion angles, there are ten unique possible conformations, which are listed in Table 4 together with their energies.

Table 4. The unique MM energy conformations for one qpy chain (torsion angles are listed successively, starting at a terminal pyridine ring)

Conformer	Energy (kcal·mol^{-1})	N−C−C−N torsion angles (°)			
tttt	114.76	180.0	179.9	180.0	180.0
ttct	114.95	−179.7	178.5	22.8	178.6
tttc	117.09	179.9	−179.3	179.2	21.7
tccc	120.32	179.9	18.9	−7.7	21.7
cctc	121.70	19.7	22.2	179.4	−21.3
tcct	116.37	−178.0	10.8	10.8	−178.0
tctc	117.99	−178.9	−23.3	−179.2	22.1
ttcc	118.76	−179.4	178.7	22.7	−20.6
cttc	119.75	−19.9	179.4	−179.4	19.9
cccc	124.89	−21.1	−19.8	14.0	−21.0

The results show that the steric energy increases with the number of *cis* torsion angles present in each conformation. Thus, the lowest energy conformation has an energy of 114.76 kcal·mol^{-1}, and exhibits a *tttt* conformation. In the crystal structure of $[H_2(qpy)][PF_6]_2$,[14] the qpy chain (model 1) exhibits a *cttc* conformation with N−C−C−N torsion angles of 3.5, 177.8, 174.5, and 6.9°. This conformation has an energy of 119.77 kcal·mol^{-1} in the gas phase but, in the crystal, two symmetry related $[H_2(qpy)]^{2+}$ cations are assembled face to face through a π-stacking arrangement with an interplanar distance ca. 3.89 Å, and by hydrogen bonding interactions involving the PF_6^- counterions and N−H groups. Therefore, the observed conformation is probably stabilized by these intermolecular interactions and avoids the low energy *tttt* conformation.

In the structure of $[Ag(qpy)][PF_6]$,[7] the qpy ligand adopts a helical shape, with four N−C−C−N torsion angles of −19.7, 1.1, 1.1, and −19.7° defining a *cccc* conformation. An energy of 125.20 kcal mol^{-1} and N−C−C−N torsion angles of −21.1, −19.8, 14.0, and −21.0° were calculated for this conformation, which is the highest energy conformation, and is forced by the binding of silver to the five nitrogen donors.

Having established the structural preferences of the monomeric chain, we then evaluated the stability of a dimeric model involving the self-assembling of two chains of qpy. The energy minimization of the supramolecular aggregate composed of two $[Fc_2(qpy)]$ units, from the X-ray structure of $[Ag_2(Fc_2qpy)_2]^{2+}$ after removing the two silver atoms, was first attempted in the Universal Force Field, parameterized for the full periodic table, using the default parameters available for $FeCp_2$ fragments. Since convergence was not achieved, a model was created by replacing the two ferrocenyl units with hydrogen atoms. This model structure was subsequently minimized by molecular mechanics calculations, and submitted to a dynamics simulation at room temperature (300 K) during 500 ps. Conformational changes were observed with torsion angles varying from −60 to 60°. Surprisingly, the two chains retained the double helical arrangement, and no *cis* to *trans* isomerization was observed. The overall conformation remained *cisoid*. The simulation was repeated for longer simulation periods of 800 and 1000 ps, respectively, and the chains kept their helical topology in both runs. This was only lost when the temperature was raised above 400 K. The changes of N−C−C−N torsion angles with time are given in Figure 6, for a simulation carried out at 500 K, together with snapshots of the most relevant structures. After the first 144.5 ps, two terminal pyridine rings from different chains experienced a conformational change from *cis* to *trans*, but the double-helix structure was retained. Subsequently, during a period of ca. 42 ps, further conformational changes occurred, until the two chains unfolded completely, adopting an almost parallel arrangement, which remained until the end of the simulation. During this period, the arrangement of the two chains changed from *ctttcttt* → *tttttttt* → *tttttttct*, but the *transoid* conformation of the eight torsion angles was retained for a considerable time. In order to evaluate the steric stability of the different arrangements observed in the molecular dynamics simulation, all the

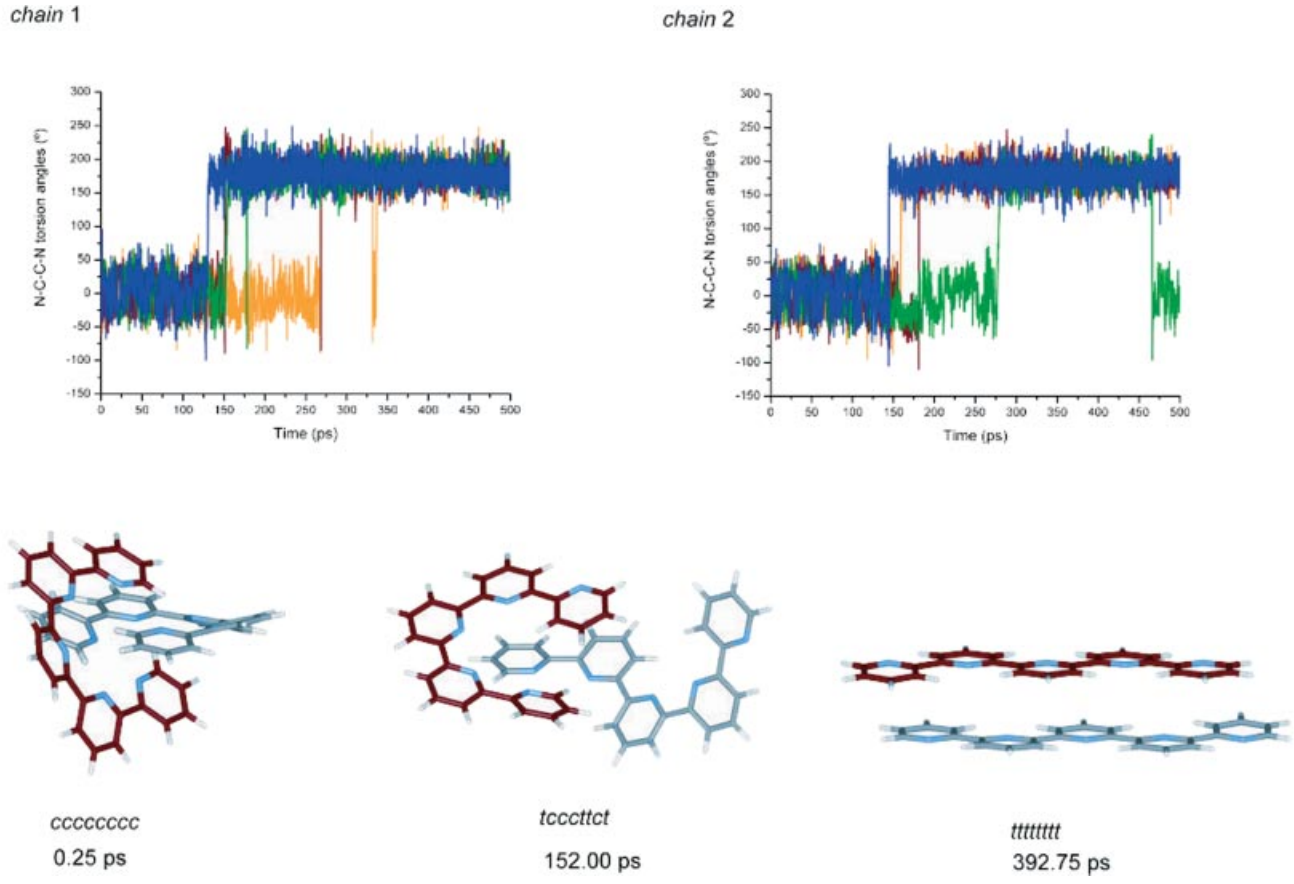

Figure 6. Changes in the N−C−C−N torsion angles during the 500 ps simulation at 500 K, with relevant snapshots showing the unfolding process of the dimeric qpy chain; the yellow, red, green, and blue curves represent the torsion angles from 2,2′, 6,2′, 6′′,2′′′, and 6′′′′, 2′′′′ C−C interannular bonds, respectively; carbon atoms of chains 1 and 2 are red and gray, respectively

frames collected were subsequently minimized by molecular mechanics (MM).

The lowest energy structure (215.94 kcal·mol^{-1}) corresponds to a *tttttttt* conformation, in which the pyridine rings of both chains are π-stacked, with the nitrogen atoms in a *trans* arrangement. In fact, the two terminal pyridine rings subtend a dihedral angle of 4.3°, and the chains are separated by a distance of ca. 3.732 Å. In other words, this supramolecular dimer is stabilized by π-π interactions.

In contrast, the double helix structure *cccccccc*, with torsion angles of −22.8, 22.1, −24.9, −18.9, −22.8, 22.1, −24.9, and −18.9°, is among those with the highest energies (223.97 kcal·mol^{-1}), as reported for the monomer. This conformation was observed in the solid state for $[Ag_2(Fc_2qpy)_2](OTf)_2$ with torsion angles of −1.8 −23.9 −35.9 −3.9 −4.8 −40.2, −28.5, and −1.8°. Therefore, in spite of the apparent stability shown by the double-helix *cccccccc* conformer in the gas phase, dynamics and mechanics results suggest that the silver atoms are, apparently, crucial for this conformational preference.

Selected geometric arrangements of the dimeric qpy chain were also optimized by DFT calculations, the results

Table 5. Low-energy MM structures resulting from self-assembling of two qpy chains

Conformer	Energy (kcal·mol^{-1})	N−C−C−N torsion angles (°)							
tttttttt	215.94	−176.1	−179.5	−178.6	176.5	−176.5	178.7	179.6	176.1
tcttttttt	219.58	174.8	13.9	179.6	178.3	−177.7	−175.4	−170.0	−178.5
tcctttttt	220.36	−175.3	−25.5	12.4	175.2	165.5	−160.1	166.9	−174.2
tcctttct	220.55	168.8	20.7	−20.8	175.5	176.8	179.6	17.3	171.7
ccctccc	220.90	15.6	−21.8	−23.7	−175.3	−175.4	−23.7	−21.8	15.6
ccccctccc	223.15	12.9	−22.4	−26.7	15.1	−168.3	−23.5	−21.4	12.2
cccccccc	223.97	−22.8	22.1	−24.9	−18.9	−22.8	22.1	−24.9	−18.9
tcttcttt	225.02	179.7	−176.6	−179.5	16.9	178.3	−165.3	24.4	175.8
ccctttttt	225.17	−18.1	14.3	11.8	−177.8	179.1	−166.7	170.2	−173.2
tccctttct	227.38	−169.4	−16.7	−11.2	15.7	−177.4	178.1	21.2	173.5
tccccctct	232.03	−176.4	−15.7	−2.4	−19.0	−22.8	−149.9	31.2	176.3

Table 6. DFT minimized conformations of the supramolecular aggregate of two qpy chains

Conformer	Relative energy (kcal·mol^{-1})	N−C−C−N torsion angles (°)							
ttttttt	0.0	−178.3	−178.9	178.4	179.6	−179.7	−178.6	179.3	177.7
tcttttt	6.6	172.3	17.7	179.1	178.6	178.9	−166.8	−179.6	−179.3
tcttcttt	15.9	173.9	30.8	−165.8	−179.5	16.6	−178.4	−177.0	−178.8
tcccctct	22.6	−174.1	−12.7	−12.6	−21.3	178.6	33.2	−158.2	26.0
cccccccc	41.1	14.6	−26.1	−26.1	14.4	13.7	−25.9	−26.2	14.1

being similar to those discussed above. The *ttttttt* conformation is again the most stable, with an energy lower than that of the *cccccccc* conformer by 44.13 kcal·mol^{-1}. The resultant structures together with their relative energies are given in Table 6.

Conclusions

Although silver helical complexes of the type described here have been known for some years, no previous theoretical evaluation has, to the best of our knowledge, been carried out. DFT calculations were performed with a relatively small model, required by the large size of the real system, but were still able to reveal the main patterns. Optimized DFT geometries were very close to those observed experimentally, both in the case of the monomeric species, and of the double helical chain complex with two silver atoms. In our model, the optimized monomer (Figure 5, b) was found to be more stable than a related complex with a helical structure (Figure 5, a). Molecular dynamics and molecular mechanics also showed that the two chains in the helix (experimental structure or DFT optimized) exhibit a high energy conformation, while the planar arrangement of two chains is stabilized by π-π stacking interactions between the aromatic rings, and it is the lowest energy one. Thus, the preference for a dimeric structure depends on the balance between the reorganization energy of the two chains, i.e. between the preferred *tttt* conformation and the high energy *cccc*, and the energy released by the formation of globally stronger Ag−N bonds and the new Ag−Ag bond. The balance of these terms, accompanied by subtle factors not considered in our models, such as packing effects or π-π stacking, will strongly depend on the substituents.

Experimental Section

Instrumentation: Infrared spectra were recorded in the range 4000−200 cm^{-1} with a Perkin−Elmer 883 spectrophotometer using nujol mulls between polyethylene sheets. Conductivities were measured in ca. 5×10^{-4} mol·dm^{-3} solutions with a Philips 9509 conductimeter. C, N, and S analyses were carried out with a Perkin−Elmer 2400 microanalyzer. Mass spectra were recorded with a VG Autospec instrument with the liquid secondary-ion mass spectra (LSIMS) technique, using nitrobenzyl alcohol as matrix. NMR spectra were recorded with a Varian Unity 300 spectrometer or a Bruker ARX 300 spectrometer in CD_2Cl_2. Chemical shifts are cited relative to $SiMe_4$ (^{1}H, external). Cyclic voltammetric experiments were performed by employing an EG&PARC model 273 potentiostat. A three-electrode system was used, which consists of a platinum disk working electrode. The measurements were carried out in CH_2Cl_2 solutions with 0.1 mol·dm^{-3} Bu_4NPF_6 as a supporting electrolyte. Under the present experimental conditions, the ferrocenium/ferrocene couple was located at 0.47 V relative to the SCE.

Synthesis of $[Ag_2(Fc_2qpy)_2](OTf)_2$: To a solution of 4′,4‴-bis-(ferrocenyl)-2,2′:6′,2″:6″,2‴:6‴,2⁗-quinquepyridine (0.075 g, 0.1 mmol) in dichloromethane (20 mL) was added AgOTf (0.026 g, 0.1 mmol), and the mixture was stirred for 1 h. Evaporation of the solvent to ca. 5 mL, and addition of hexane gave $[Ag_2(Fc_2qpy)_2](OTf)_2$ as an orange-red solid. Yield 89 %. Δ_M 110 Ω^{-1} cm^2·mol^{-1}. $C_{92}H_{66}Ag_2F_6Fe_4N_{10}O_6S_2$ (2024.836): calcd. C 54.57, H 3.28, N 6.91, S 3.16; found C 54.19, H 3.14, N 6.85, S 3.09. ^{1}H NMR: δ = 4.12 (br. m, 10 H, C_5H_5), 4.63 (br. m, 4 H, C_5H_4), 4.95 (br. m, 4 H, C_5H_4), 6.89 (m, 2 H, 5 and 5⁗ of qpy), 7.15 (m, 2 H, 4 and 4⁗ pd qpy), 7.33 (m, 1 H, 4″), 7.6−8.8 (br. m, 10 H, qpy) ppm.

Crystal Data for $[Ag_2(Fc_2qpy)_2](OTf)_2·3CH_2Cl_2$: Empirical formula $C_{95}H_{72}Ag_2Cl_6F_6Fe_4N_{10}O_6S_2$, M = 2279.59, triclinic, space group $P(-1)$, a = 14.917(3), b = 16.205(3), c = 20.572(4) Å, α = 99.71(2), β = 105.46(2), γ = 103.86(2)°, U = 4507.4(15) Å^3, Z = 2, $D_{calcd.}$ = 1.680 Mg·m^{-3}, λ(Mo-K_α) = 0.07173 Å, μ = 1.351 mm^{-1}, F(000) = 2292, T = −130 °C, orange prism, 0.35 × 0.20 × 0.20 mm. 12234 intensities were recorded to $2\theta_{max.}$ 45° (Siemens P4 diffractometer), of which 11739 were unique (R_{int} = 0.0589) after absorption corrections using SHELXA. The structure was solved by heavy-atom methods, and subjected to full-matrix least-squares refinement on F^2 (program SHELXL-97).[44] All non-hydrogen atoms were refined anisotropically. H atoms were included using a riding model. Refinement proceeded to $wR(F^2)$ 0.2101, conventional $R(F)$ 0.0743 for 1180 parameters and 2254 restraints (to light atom U values and local ring geometry), $S(F^2)$ = 0.827; maximum Δρ = 1.384 e·Å^{-3}. CCDC-218940 contains the supplementary crystallographic data for this paper. These data can be obtained free of charge at www.ccdc.cam.ac.uk/conts/retrieving.html [or from the Cambridge Crystallographic Data Center, 12 Union Road, Cambridge CB2 1EZ, UK; Fax: +44-1223/336-033; E-mail: deposit@ccdc.cam.ac.uk].

Computational Details: Density functional calculations[34] were carried out with the Amsterdam Density Functional program (ADF-2000).[35] The Local Spin Density (LSD) exchange correlation potential was used with the Local Density Approximation of the correlation energy (Vosko, Wilk and Nusair's).[45] Gradient corrected geometry optimizations,[46] without symmetry constrains, were performed using the Generalized Gradient Approximation (Becke's non-local exchange[47] and Perdew's correlation corrections).[48] A triple-ζ Slater-type orbital (STO) basis set was used for all atoms, augmented by one polarization function. A frozen core approximation was used to treat the core electrons: (1s) for N and C; ([1−3]s [2−3]p 3d) for Ag.

Single point calculations at the Hartree−Fock (HF)[49] and second order Møller−Plesset (MP2)[37] levels were performed on the ADF optimized geometries using Gaussian 98.[36] The standard LanL2DZ basis set was used for all atoms.[50] A Natural Population (NPA) analysis,[38] and the evaluation of the Wiberg indices[39] (using the MP2 density) were used as bond strength indicators. Mayer indices were calculated with the ADF densities.[40,41]

HF structure optimizations were also performed, but the agreement between calculated and experimental data was worse than that obtained with the DFT methods (longer distances, especially Ag···Ag). They were, therefore, not considered in further single point energy calculations.

The molecular dynamics simulations and mechanics calculations were carried out using the Cerius2 software[43] with parameters from the Universal Force Field.[42] The atomic charges were calculated with the Qeq method implemented in Cerius2. The conformational analysis of model 1 was performed via quench dynamics techniques. A molecular dynamics run was carried out using a time step of 1 fs and 2000 conformations were generated at 0.25 ps intervals at 3000 K. Concomitantly, the generated conformations were minimized by molecular mechanics calculations. The dynamics simulations with model 2 were carried out at temperatures of 300, 400, and 500 K, respectively, using a time step of 1fs, and a set of atomic positions were saved every 0.25 ps over the entire period of the simulation of 500 ps. The simulation runs at 300 and 400 K were repeated for 800 and 1000 ps. An NVT thermostat was used for all simulations. The structures collected in dynamics run at 500 K were subsequently minimized by molecular mechanics.

Acknowledgments

We thank the Dirección General de Investigación Científica y Técnica (No. BQU2001−2409-C02-C01) and the Fonds der Chemischen Industrie for financial support. We thank Acções-Integradas Luso-Espanholas for a bilateral project.

[1] J. M. Lehn, *Supramolecular Chemistry*, Wiley-VCH, Weinheim, **1995**.
[2] I. Haiduc, F. T. Edelmann, *Supramolecular Organometallic Chemistry*, Wiley-VCH, Weinheim, **1999**.
[3] E. C. Constable, *Prog. Inorg. Chem.* **1994**, *42*, 67.
[4] E. C. Constable, in *Comprehensive Supramolecular Chemistry*, vol. 9 (Ed.: J. M. Lehn), Pergamon, Oxford, **1996**, p. 213.
[5] M. Munakata, L. P. Wu, T. Kuroda-Sowa, *Adv. Inorg. Chem.* **1999**, *46*, 173.
[6] C. Piguet, G. Bernardinelli, G. Hopfgartner, *Chem. Rev.* **1997**, *97*, 2005.
[7] E. C. Constable, M. G. B. Drew, G. Forsyth, M. D. Ward, *J. Chem. Soc., Chem. Commun.* **1988**, 1450.
[8] E. C. Constable, J. Lewis, M. Schröder, *Polyhedron* **1982**, *1*, 311.
[9] E. C. Constable, M. G. B. Drew, M. D. Ward, *J. Chem. Soc., Chem. Commun.* **1987**, 1600.
[10] M. Barley, E. C. Constable, S. A. Corr, R. C. S. McQueen, J. C. Nutkins, M. D. Ward, M. G. B. Drew, *J. Chem. Soc., Dalton Trans.* **1988**, 2655.
[11] E. C. Constable, M. D. Ward, M. G. B. Drew, G. A. Forsyth, *Polyhedron* **1989**, *8*, 2551.
[12] E. C. Constable, S. M. Elder, J. Healy, M. D. Ward, D. A. Tocher, *J. Am. Chem. Soc.* **1990**, *112*, 4590.
[13] E. C. Constable, S. M. Elder, P. R. Raithby, M. D. Ward, *Polyhedron* **1991**, *10*, 1395.
[14] E. C. Constable, S. M. Elder, J. V. Walker, P. D. Wood, D. A. Tocher, *J. Chem. Soc., Chem. Commun.* **1992**, 229.
[15] E. C. Constable, J. V. Walker, D. A. Tocher, M. A. M. Daniels, *J. Chem. Soc., Chem. Commun.* **1992**, 768.
[16] E. C. Constable, J. V. Walker, *J. Chem. Soc., Chem. Commun.* **1992**, 884.
[17] E. C. Constable, M. A. M. Daniels, M. G. B. Drew, D. A. Tocher, J. V. Walker, P. D. Wood, *J. Chem. Soc., Dalton Trans.* **1993**, 1947.
[18] E. C. Constable, R. Martínez-Máñez, A. M. W. Cargill Thompson, J. V. Walker, *J. Chem. Soc., Dalton Trans.* **1994**, 1585.
[19] E. C. Constable, A. J. Edwards, P. R. Raithby, J. V. Walker, *Angew. Chem. Int. Ed. Engl.* **1993**, *32*, 1465.
[20] P. K. K. Ho, K. K. Cheung, C. M. Che, *Chem. Commun.* **1996**, 1197.
[21] P. K. K. Ho, K. K. Cheung, S. M. Peng, C. M. Che, *J. Chem. Soc., Dalton Trans.* **1996**, 1411.
[22] Y. Fu, Q. Li, Z. Zhou, W. Dai, D. Wang, T. C. W. Mak, H. Hu, W. Tang, *Chem. Commun.* **1996**, 1549.
[23] E. C. Constable, A. J. Edwards, P. R. Raithby, D. R. Smith, J. V. Walker, L. Whall, *Chem. Commun.* **1996**, 2551.
[24] E. C. Constable, M. Neuburger, L. A. Whall, M. Zehnder, *New J. Chem.* **1998**, *22*, 219.
[25] C. J. Cathey, E. C. Constable, M. J. Hannon, D. A. Tocher, M. D. Ward, *J. Chem. Soc., Chem. Commun.* **1990**, 621.
[26] E. C. Constable, C. J. Cathey, M. J. Hannon, D. A. Tocher, J. V. Walker, M. D. Ward, *Polyhedron* **1999**, *18*, 159.
[27] E. C. Constable, J. V. Walker, *Polyhedron* **1998**, *17*, 3089.
[28] K. T. Potts, M. Keshavarz, K. F. S. Than, H. D. Abruna, C. R. Arana, *Inorg. Chem.* **1993**, *32*, 4422.
[29] K. T. Potts, M. Keshavarz, K. F. S. Than, H. D. Abruna, C. R. Arana, *Inorg. Chem.* **1993**, *32*, 4436.
[30] W. Dai, H. Hu, X. Wei, X. Zhu, D. Wang, K. Yu, N. R. Dalley, X. Kou, *Polyhedron* **1997**, *16*, 2059.
[31] Y. Fu, J. Sun, Q. Li, Y. Chen, W. Dai, D. Wang, T. C. W. Mak, W. Tang, H. Hu, *J. Chem. Soc., Dalton Trans.* **1996**, 2309.
[32] E. C. Constable, S. M. Elder, M. J. Hannon, A. Martin, P. R. Raithby, D. A. Tocher, *J. Chem. Soc., Dalton Trans.* **1996**, 2423.
[33] G. Baum, E. C. Constable, D. Fenske, C. E. Housecroft, T. Kulke, *Chem. Commun.* **1998**, 2659.
[34] R. G. Parr, W. Yang, *Density Functional Theory of Atoms and Molecules*, Oxford, University Press, New York, **1989**.
[35] [35a] *ADF-2000*: E. J. Baerends, A. Bérces, C. Bo, P. M. Boerrigter, L. Cavallo, L. Deng, R. M. Dickson, D. E. Ellis, L. Fan, T. H. Fischer, C. Fonseca Guerra, S. J. A. van Gisbergen, J. A. Groeneveld, O. V. Gritsenko, F. E. Harris, P. van den Hoek, H. Jacobsen, G. van Kessel, F. Kootstra, E. van Lenthe, V. P. Osinga, P. H. T. Philipsen, D. Post, C. C. Pye, W. Ravenek, P. Ros, P. R. T. Schipper, G. Schreckenbach, J. G. Snijders, M. Sola, D. Swerhone, G. te Velde, P. Vernooijs, L. Versluis, O. Visser, E. van Wezenbeek, G. Wiesenekker, S. K. Wolff, T. K. Woo, T. Ziegler. [35b] C. Fonseca Guerra, O. Visser, J. G. Snijders, G. te Velde, E. J. Baerends, *Parallelisation of the Amsterdam Density Functional Program in: Methods and Techniques for Computational Chemistry* (Eds.: E. Clementi, C. Corongiu), p. 303−395, STEF, Cagliari, **1995**. [35c] C. Fonseca Guerra, J. G. Snijders, G. te Velde, E. J. Baerends, *Theor. Chem. Acc.* **1998**, *99*, 391. [35d] E. J. Baerends, D. Ellis, P. Ros, *Chem. Phys.* **1973**, *2*, 41. [35e] E. J. Baerends, P. Ros, *Int. J. Quantum Chem.* **1978**, *S12*, 169. [35f] P. M. Boerrigter, G. te Velde, E. J. Baerends, *Int. J. Quantum Chem.* **1988**, *33*, 87. [35g] G. te Velde, E. J. Baerends, *J. Comp. Phys.* **1992**, *99*, 84.
[36] *Gaussian 98* (Revision A.7): M. J. Frisch, G. W. Trucks, H. B. Schlegel, G. E. Scuseria, M. A. Robb, J. R. Cheeseman, V. G. Zakrzewski, J. A. Montgomery, R. E. Stratmann, J. C. Burant, S. Dapprich, J. M. Millam, A. D. Daniels, K. N. Kudin, M. C. Strain, O. Farkas, J. Tomasi, V. Barone, M. Cossi, R. Cammi, B. Mennucci, C. Pomelli, C. Adamo, S. Clifford, J. Ochterski, G. A. Petersson, P. Y. Ayala, Q. Cui, K. Morokuma, D. K. Malick, A. D. Rabuck, K. Raghavachari, J. B. Foresman, J. Cioslowski, J. V. Ortiz, B. B. Stefanov, G. Liu, A. Liashenko, P. Piskorz, I. Komaromi, R. Gomperts, R. L. Martin, D. J. Fox, T. Keith, M. A. Al-Laham, C. Y. Peng, A. Nanayakkara, C.

Gonzalez, M. Challacombe, P. M. W. Gill, B. G. Johnson, W. Chen, M. W. Wong, J. L. Andres, M. Head-Gordon, E. S. Replogle, J. A. Pople, Gaussian, Inc., Pittsburgh, PA, **1998**.
[37] [37a] C. Møller, M. S. Plesset, *Phys. Rev.* **1934**, *46*, 618. [37b] J. S. Binkley, J. A. Pople, *Int. J. Quantum Chem.* **1975**, *9*, 229. [37c] J. S. Binkley, J. A. Pople, R. Seeger, *Int. J. Quantum Chem.* **1976**, *S10*, 1. [37d] R. Krishnan, J. A. Pople, *Int. J. Quantum Chem.* **1978**, *14*, 91. [37e] R. Krishnan, M. Frisch, J. A. Pople, *J. Chem. Phys.* **1980**, *72*, 4244.
[38] [38a] J. E. Carpenter, F. Weinhold, *Mol. Struct. (Theochem)* **1988**, *169*, 41. [38b] J. E. Carpenter, *PhD Thesis, University of Wisconsin (Madison WI)*, **1987**. [38c] J. P. Foster, F. Weinhold, *J. Am. Chem. Soc.* **1980**, *102*, 7211. [38d] A. E. Reed, F. Weinhold, *J. Chem. Phys.* **1983**, *78*, 4066. [38e] A. E. Reed, F. Weinhold, *J. Chem. Phys.* **1983**, *78*, 1736. [38f] A. E. Reed, R. B. Weinstock, F. Weinhold, *J. Chem. Phys.* **1985**, *83*, 735. [38g] A. E. Reed, L. A. Curtiss, F. Weinhold, *Chem. Rev.* **1988**, *88*, 899. [38h] F. Weinhold, J. E. Carpenter, *The Structure of Small Molecules and Ions*, Plenum, **1988**, 227.
[39] K. B. Wiberg, *Tetrahedron* **1968**, *24*, 1083.
[40] I. Mayer, *Chem. Phys. Lett.* **1983**, *97*, 270; I. Mayer, *Int. J. Quantum Chem.* **1984**, *26*, 151.
[41] *MAYER*: A. J. Bridgeman, C. J. Empson, University of Hull (**2002**). Freely available on the worldwide web from http://www.hull.ac.uk/php/chsajb/mayer/.
[42] A. K. Rappe, C. J. Casewit, K. S. Colwell, W. A. Goddard III, W. M. Skiff, *J. Am. Chem. Soc.* **1992**, *114*, 10024.
[43] *CERIUS2*, version 4.2, Molecular Simulations Inc, San Diego, **2000**.
[44] G. M. Sheldrick, *SHELXL-97, A Program for Crystal Structure Refinement*, University of Göttingen, **1997**.
[45] S. H. Vosko, L. Wilk, M. Nusair, *Can. J. Phys.* **1980**, *58*, 1200.
[46] [46a] L. Versluis, T. Ziegler, *J. Chem. Phys.* **1988**, *88*, 322. [46b] L. Fan, T. Ziegler, *J. Chem. Phys.* **1991**, *95*, 7401.
[47] A. D. Becke, *Phys. Rev. A.* **1988**, *38*, 3098.
[48] J. P. Perdew, *Phys. Rev. B.* **1986**, *33*, 8822.
[49] W. J. Hehre, L. Radom, P. v. R. Schleyer, J. A. Pople, *Ab Initio Molecular Orbital Theory*, John Wiley & Sons, New York, **1986**.
[50] [50a] T. H. Dunning, Jr., P. J. Hay, *Modern Theoretical Chemistry* (Ed.: H. F. Schaefer III), Plenum, New York, **1976**, vol. 3, p. 1. [50b] P. J. Hay, W. R. Wadt, *J. Chem. Phys.* **1985**, *82*, 270. [50c] W. R. Wadt, P. J. Hay, *J. Chem. Phys.* **1985**, *82*, 284. [50d] P. J. Hay, W. R. Wadt, *J. Chem. Phys.* **1985**, *82*, 2299.

Received January 22, 2004
Early View Article
Published Online June 1, 2004

